Fairness-Constrained Rate Optimization of Multi-Link Slotted Aloha

Wen Zhan, *Member, IEEE*, Buwei Wu, Xinghua Sun, *Member, IEEE*, Kai Xie, and Xiang Chen, *Member, IEEE*

***Abstract*—This letter optimizes the data rate performance of multi-link slotted Aloha networks, in which Multi-Link Devices (MLDs) coexist with multiple groups of Single-Link Devices (SLDs), where different groups reside in distinct channels. MLDs can transmit/receive packets via multiple channels, causing interference to all groups of SLDs and severe rate unfairness issue. To ensure SLDs in different channels can acquire target ratios of data rate, explicit expressions of sum rate and group data rate are derived, based on which the optimal transmission probabilities of MLDs/SLDs for maximizing the sum rate without or with fairness constraints are obtained. The analysis reveals the coupling effect of the behavior of devices in different channels, the tradeoff between the optimal sum rate performance and the fairness, and the effect of channel fading on benefit of using multi-link transmission capability.**

***Index Terms*—Multi-Link, slotted Aloha, sum rate, fairness constraint.**

I. Introduction

With the rapid development of the Internet of Things (IoT) industry, millions of smart devices step into our daily life and require pervasive wireless connectivity with distinct Quality of Service (QoS) demands [1]. To accommodate massive access requests from uncoordinated low-cost devices, the classical random access scheme, slotted Aloha [2], has been regarded as an appealing solution and widely used in existing wireless communication systems to support IoT services [3], [4].

To boost the throughput performance, practical networks, such as NB-IoT [3], put the multi-channel transmission into consideration, with which each node can transmit packets in a randomly selected channel. Yet, for each node, at most one packet can be successfully delivered in each time slot even with multiple channels, because it has only one radio (air-interface) for transmission and reception. The demand for high throughput in IoT services motivates the multi-link technology [5], where Multi-Link Devices (MLD), each of which configures multiple radios inside, can transmit/receive packets over multiple channels at the same time and obtain better rate performance than that in the single-radio case.

To release the full potential of multi-link operation, Simultaneous Transmission and Reception (STR) capability is the ideal solution, where each MLD performs reception on some channels while simultaneously transmitting packets on other channels. Yet, the STR capability is subject to a variety of factors of radio design including transmit power limit and antenna distribution between the channels, etc, such that MLDs may lack the STR capability [6]. In this case, a common strategy for coordinating the transceiver operation of MLDs is all radios of each MLD transmit or receive packets at the same time [7].

To be more specific, in multi-link[1] slotted Aloha network, all radios in each MLD could send packets in multiple channels simultaneously with a certain probability in each time slot. The behaviour of each MLD affects the transmission outcomes in all channels that it can use. Yet, in classical multi-channel slotted Aloha network, each node can access only one channel and the behavior of each node in a channel is independent of the contention process in other channels. As a result, the performance analysis of the multi-link slotted Aloha network does not follow that for classical multi-channel slotted Aloha in [8], [9], [10], [11]. In [5] and [12], the throughput performance of multi-link IEEE 802.11be networks was evaluated in the context of carrier sense multiple access protocol. Yet, there has been no research work on the throughput or rate performance of the multi-link slotted Aloha networks.

Moreover, it is intuitively clear that the MLD takes advantage over SLD in that MLD can access multiple channels at the same time and achieves better rate performance. However, this advantage is achieved at the cost of mounting channel interference to SLDs in different channels and degraded rate performance of SLDs. The QoS of SLDs may not be guaranteed and a fairness issue arises. Considering that SLDs and MLDs may coexist in the same network, how to optimize the network sum rate performance under the constraint of providing a QoS guarantee to SLDs is of great importance.

This letter aims to address the above open issues in a multi-link slotted Aloha network which consists of one multi-link group and multiple single-link groups, and each MLD in the multi-link group can access all channels. Due to distinct channel fading conditions, the information encoding rates

Manuscript received 19 November 2022; accepted 1 January 2023. Date of publication 9 January 2023; date of current version 3 March 2023. This work was supported in part by the Key-Area Research and Development Program of Guangdong Province under Grant 2019B010158001; in part by the National Natural Science Foundation of China under Grant 62001524; and in part by the Shenzhen Science and Technology Program under Grant RCBS20210706092408010. The associate editor coordinating the review of this article and approving it for publication was O. M. Caicedo Rendon. *(Corresponding authors: Kai Xie; Xinghua Sun.)*

Wen Zhan, Buwei Wu, Xinghua Sun, and Kai Xie are with the School of Electronics and Communication Engineering, Shenzhen Campus of Sun Yat-sen University, Shenzhen 518107, China (e-mail: zhanw6@mail.sysu.edu.cn; wubw7@mail2.sysu.edu.cn; sunxinghua@mail.sysu.edu.cn; xiek8@mail.sysu.edu.cn).

Xiang Chen is with the School of Electronics and Information Technology, Sun Yat-sen University, Guangzhou 510275, Guangdong, China (e-mail: chenxiang@mail.sysu.edu.cn).

Digital Object Identifier 10.1109/LNET.2023.3235404

[1]In this letter, the channel refers to a specific division of frequencies for sending and receiving data and the link refers to a communication bearer consisting of a pair of transmitter and receiver in a channel.

in different links are different. By characterizing the behavior of the HoL (Head-of-Line) of each device, the maximum network sum rate with/without fairness constraints and the corresponding optimal transmission probabilities of each device are obtained as the explicit functions of the number of devices in each group and the encoding rate in each channel, where the fairness constraint is measured by the ratio of the group rate of the single-link group to that of the multi-link group in each channel.

The analysis shows that due to the effect of the behavior of MLDs, the optimal transmission probabilities of all groups in different channels are closely correlated. With fairness constraint, the maximum sum rate has to be sacrificed and the degradation becomes severe as the fairness requirements of single-link groups differ widely. The effect of channel fading conditions on the data rate performance is also revealed, which sheds important insights for practical multi-link system design.

The remainder of this letter is organized as follows. Section II presents the system model and preliminary analysis. The maximum network sum rate without and with fairness constraints, along with the optimal transmission probabilities of each group, are characterized in Section III. Finally, conclusions are summarized in Section IV.

II. System Model and Preliminary Analysis

A. System Model

This letter considers a multi-link slotted Aloha network, as shown in Fig. 1, which contains channel $c \in \{1, \ldots, L\}$ and Group $g, g \in \{1, 2, \ldots, L, M\}$, where L denotes the amount of channels and M represents multi-link group. The size of each group is denoted by $n^{(g)}$. Among those $L+1$ groups, Group $c, c \in \{1, 2, \ldots, L\}$ is the single-link group, in which each device can access channel c only. While, Group M is the multi-link group, in which devices have multiple radios such that they transmit packets in all L channels.

The saturated condition is considered, where each device always has packets to send. With the classic collision model, if more than one devices send data packets at the same time slot in the same channel, then a collision occurs and packet transmission fails. To control the channel contention, each device in Group $g, g \in \{1, 2, \ldots, L, M\}$ would set its transmission probability as $q^{(g)} \in (0, 1)$. Similar to [6], [7], we assume that MLDs lack the STR capability and all radios transmit/receive packets at the same time.

Note that the physical attributes of a wireless channel, such as fading and path loss, would affect the data transmission. For overcoming such effect, the modulation and coding scheme should be properly adopted, which further determines the encoding rate of each packet. To capture the essence of channel effect without involving details of physical attributes of wireless channel,[2] we assume the encoding rate of each packet in channel c, denoted by R_c bit/s/Hz, has been carefully selected for reliable communication [13].

[2]The encoding rate depends on the transmission power, small/large scale fading, transmitter-receiver distance, etc. The analysis can be extended to incorporate those channel effects by further including a wireless channel fading model.

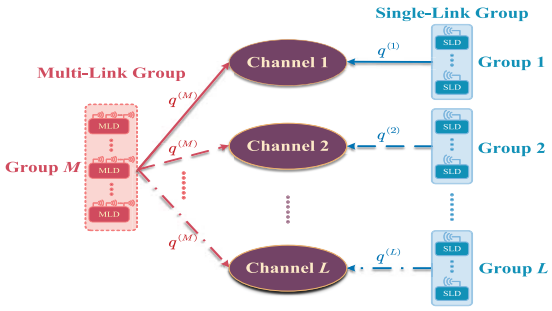

Fig. 1. $L+1$ groups of nodes share L channels. Group M is the multi-link group. Group $c, c \in \{1, 2, \ldots, L\}$ is the single-link group.

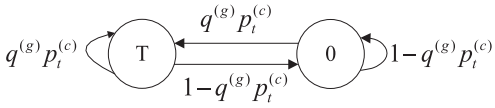

Fig. 2. State transition diagram of each individual HoL packet of nodes in Group $g \in \{1, 2, \ldots, L, M\}$ at the channel $c \in \{1, 2, \ldots, L\}$.

Let $N_t^{(g,c)}$ denote the total number of successfully-decoded packets from Group g over channel c in time slot t. The group throughput, denoted as the long-term average amount of successful transmission packets of each device group, can then be defined as $\hat{\lambda}_{out}^{(g)} \triangleq \lim_{t\to\infty} \frac{1}{t} \sum_{i=1}^{t} \sum_{c=1}^{L} N_i^{(g,c)}$. With the information encoding rate of R_c in each channel, the average received information rate of each group $R_{out}^{(g)}, g \in \{1, 2, \ldots, L, M\}$ can be written as

$$R_{out}^{(c)} = R_c \cdot \hat{\lambda}_{out}^{(c)} \text{ and } R_{out}^{(M)} = \sum_{c=1}^{L} R_c \cdot \hat{\lambda}_{out}^{(M,c)}, \quad (1)$$

for $c \in \{1, 2, \ldots, L\}$, where $\hat{\lambda}_{out}^{(M,c)}$ denotes the group data rate of the multi-link group in channel c.

B. Modeling and Rate Analysis

This subsection characterizes the behavior of the HoL packet of each device and the rate performance.

The behavior of the HoL packet of each node can be characterized based on the discrete-time Markov process established in [14]. Geometric retransmission is considered, where State T denotes the successful transmission state and State 0 denotes the waiting state. As Fig. 2 shows, a fresh HoL packet is initially in State T and moves back to State T if it is successfully transmitted. Otherwise, it moves to State 0 and finally shifts to State T upon successful transmission. The steady-state probability distribution of the Markov chain in Fig. 2 can be obtained as

$$\pi_T^{(g)} = q^{(g)} p^{(c)} \text{ and } \pi_0^{(g)} = \frac{1-q^{(g)}p^{(c)}}{q^{(g)}p^{(c)}} \pi_T^{(g)}, \quad (2)$$

where $p^{(c)} = \lim_{t\to\infty} p_t^{(c)}$ is the steady-state probability of successful transmission of packets in channel $c \in \{1, 2, \ldots, L\}$. $\pi_T^{(g)}$ is the service rate of each queue in Group g. In channel $c \in \{1, \ldots, L\}$, for any given device of Group $g \in \{c, M\}$, its HoL packet transmission is successful if and only if all other devices from Group M and Group c do not request

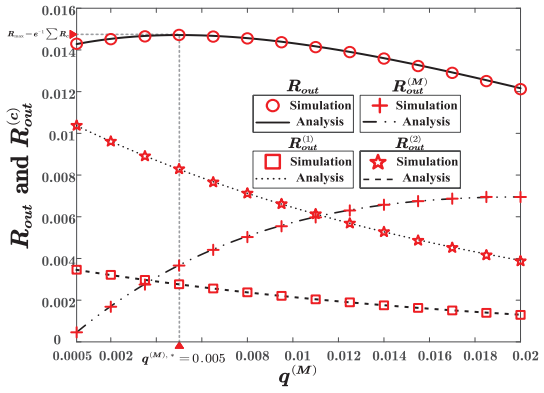

Fig. 3. Network sum rate R_{out} and the group rate $R_{out}^{(g)}, g \in \{1, 2, M\}$ versus the transmission probability of group M, $q^{(M)}$. $n^{(1)} = 50, n^{(2)} = 75, n^{(M)} = 50$. $q^{(2),*} = \frac{n^{(1)} q^{(1)}}{n^{(2)}}$. $q^{(1),*} = 0.0015$. $L = 2$. $R_1 = 0.01$ bit/s/Hz. $R_2 = 0.03$ bit/s/Hz.

transmission. Therefore, $p^{(c)}$ is given by

$$p^{(c)} = \prod_{g \in \{c, M\}} \left(1 - (\pi_T^{(g)} q^{(g)} + \pi_0^{(g)} q^{(g)})\right)^{n^{(g)}} \approx \exp\left(-n^{(c)} q^{(c)} - n^{(M)} q^{(M)}\right), \quad (3)$$

according to (2) and approximating $(1-x)^n \approx \exp(-nx)$ for $0 < x < 1$, and $n - 1 \approx n$ for a large n.

In the saturated condition, the node throughput equals the service rate of its data queue. Therefore, the group throughput can be written as $\hat{\lambda}_{out}^{(c)} = n^{(c)} p^{(c)} q^{(c)}$, for $c \in \{1, 2, \ldots, L\}$ and $\hat{\lambda}_{out}^{(M)} = n^{(M)} q^{(M)} \sum_{i=1}^{L} p^{(i)}$, based on which the data rate of each group could be further written as

$$R_{out}^{(c)} = \begin{cases} n^{(c)} p^{(c)} q^{(c)} R_c, & \text{for } c \in \{1, 2, \ldots, L\} \\ n^{(M)} q^{(M)} \sum_{i=1}^{L} p^{(i)} R_i, & \text{for } c = M, \end{cases} \quad (4)$$

and the network sum data rate as

$$R_{out} = \sum_{c=1}^{L} n^{(c)} q^{(c)} p^{(c)} R_c + n^{(M)} q^{(M)} \sum_{c=1}^{L} p^{(c)} R_c. \quad (5)$$

III. Rate Optimization

This section optimizes the sum rate by tuning the transmission probability of each group without/with fairness constraint.

A. Sum Rate Optimization

Define the maximum sum rate of the multi-link slotted Aloha network as $R_{\max} = \max_{q^{(g)}, g \in \{1,2,\ldots,L,M\}} R_{out}$. The following theorem presents $R_{\max}$ and the corresponding optimal transmission probability of each group $q^{(g),*}, g \in \{1, 2, \ldots, L, M\}$.

Theorem 1: The maximum sum rate of the multi-link slotted Aloha network $R_{\max} = e^{-1} \sum_{c=1}^{L} R_c$ is achieved if and only if the transmission probabilities of nodes in all groups satisfy

$$n^{(c)} q^{(c),*} + n^{(M)} q^{(M),*} = 1, \quad (6)$$

where $c \in \{1, 2, \ldots, L\}$.

Proof: By combining (1)–(3), (4)–(5) and approximating $x + 1 \approx x$ for large x, we can rewrite (5) as $R_{out} = -\sum_{c=1}^{L} p^{(c)} \ln p^{(c)} R_c$, from which we can see that the sum rate R_{out} is maximized at $R_{\max} = e^{-1} \sum_{c=1}^{L} R_c$ with $p^{(c)} = e^{-1}, c \in \{1, 2, \ldots, L\}$. By substituting $p^{(c)} = e^{-1}, c \in \{1, 2, \ldots, L\}$ into (3), we can obtain (6). ■

Theorem 1 shows that to achieve $R_{\max}$, the transmission probabilities of all groups should be jointly tuned according to the group sizes such that for each channel, only one packet is transmitted in each time slot on average. In addition, due to the coupling among groups, it can be obtained from (6) that for any two single-link groups, we have $n^{(i)} q^{(i),*} = n^{(c)} q^{(c),*}, i, c \in \{1, 2, \ldots, L\}$, implying that given group size $n^{(k)}, k \in \{1, 2, \ldots, L, M\}$ and the transmission probability of any group k, then the optimal transmission probabilities of all other groups $j, j \in \{1, 2, \ldots, M, L\}/k$ can be determined.

Fig. 3 demonstrates how the sum rate R_{out} and the group rate $R_{out}^{(g)}, g \in \{1, 2, M\}$ vary with the transmission probability of the multi-link group $q^{(M)}$ with $R_1 = 0.001$ bit/s/Hz and $R_2 = 0.003$ bit/s/Hz. The simulation setting is the same as the system model described in Section II and therefore, the details are omitted. We can see from Fig. 3 that with the optimal settings according to Theorem 1, the maximum sum rate is achieved, with which we can further derive the group rate of each single-link group as

$$R_{out}^{(c)} = R_c (1 - n^{(M)} q^{(M),*}) e^{-1}, c \in \{1, 2, \ldots, L\}, \quad (7)$$

according to Theorem 1 and (4). It indicates that with $R_{out} = R_{\max}$, the group data rate of each single-link group is determined by the number of nodes of the multi-link group $n^{(M)}$ and the transmission probability of the multi-link group $q^{(M),*}$. As shown in Fig. 3, with a large $q^{(M),*}$, the group data rate of the multi-link group $R_{out}^{(M)}$ increases, yet, at the cost of the group data rate of each single-link group $R_{out}^{(c)}$, $c \in \{1, 2, \ldots, L\}$, clearly indicating a severe fairness issue.

B. Fairness-Constrained Rate Optimization

In practice, however, many applications may have requirements on the rate performance [15]. The QoS requirements would not be satisfied if the rate is too small. Thus, in this section, we further study how to maximize the sum rate with rate fairness constraint. Without loss of generality, define the rate fairness constraint as the proportional relationship between the group rate of the single-link group and that of the multi-link group, i.e., $\frac{R_{out}^{(c)}}{R_{out}^{(M,c)}}, c \in \{1, 2, \ldots, L\}$, where $R_{out}^{(M,c)} \triangleq R_c \hat{\lambda}_{out}^{(M,c)}$ denotes the rate of the multi-link group in channel c.

Let $R_{\max}^F$ denotes the maximum sum rate with fairness constraints. We will address the optimization problem below

$$R_{\max}^F = \max_{q^{(g)}, g \in \{1,2,\ldots,L,M\}} R_{out}, \quad \text{s.t. } \frac{R_{out}^{(c)}}{R_{out}^{(M,c)}} = \beta^{(c)}, c \in \{1, 2, \ldots, L\}, \quad (8)$$

where $\beta^{(c)}$ is the required fairness ratio in channel c. The following theorem presents $R_{\max}^F$, and the corresponding

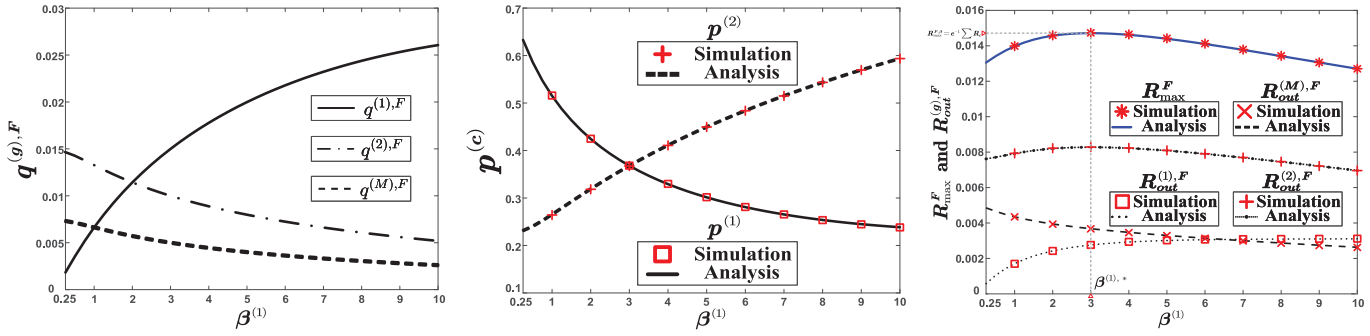

Fig. 4. (a) Optimal transmission probability of each group $q^{(g),F}, g \in \{1, 2, M\}$ versus the fairness ratio of channel 1 $\beta^{(1)}$. (b) Successful transmission probability of each channel $p^{(c)}, c \in \{1, 2\}$ versus $\beta^{(1)}$. (c) Fairness-constrained data rate of each group $R_{out}^{(g),F}, g \in \{1, 2, M\}$ and maximum network sum rate $R_{\max}^{F}$ versus $\beta^{(1)}$. $\beta^{(2)} = 3$. $n^{(1)} = 50, n^{(2)} = 75, n^{(M)} = 50$. $R_1 = 0.01$ bit/s/Hz. $R_2 = 0.03$ bit/s/Hz.

optimal transmission probability of each group $q^{(g),F}, g \in \{1, 2, \ldots, L, M\}$.

Theorem 2: The fairness-constrained maximum sum rate

$$R_{\max}^{F} = \frac{\sum_{c=1}^{L} \Gamma(\beta^{(c)}, q^{(M)}) \cdot \sum_{c=1}^{L} \left[\Gamma(\beta^{(c)}, q^{(M)}) \cdot R_c\right]}{\sum_{c=1}^{L} (1+\beta^{(c)})^2 \exp\left[-\beta^{(c)} n^{(M)} q^{(M),F}\right]}, \tag{9}$$

is achieved if and only if the transmission probabilities satisfy

$$\begin{cases} q^{(M),F} = \dfrac{\sum_{c=1}^{L} (1+\beta^{(c)}) \exp\left[-\beta^{(c)} n^{(M)} q^{(M),F}\right]}{n^{(M)} \sum_{c=1}^{L} (1+\beta^{(c)})^2 \exp\left[-\beta^{(c)} n^{(M)} q^{(M),F}\right]}, \\ q^{(c),F} = \dfrac{\beta^{(c)} n^{(M)}}{n^{(c)}} q^{(M),F}, c \in \{1, 2, \ldots, L\}, \end{cases} \tag{10}$$

where $\Gamma(\beta^{(c)}, q^{(M)}) = (1 + \beta^{(c)}) \exp\left[-\beta^{(c)} n^{(M)} q^{(M),F}\right]$.

Proof: The Lagrangian multiplier method is used for solving the constrained optimization problem in (8). The details are omitted due to limited space. ■

By comparing Theorem 1 and Theorem 2, we can see that in sharp contrast to (6), when the fairness constraint is taken into consideration, the optimal transmission probability of the multi-link group $q^{(M),F}$ no longer depends on the number of nodes of single-link groups. Instead, it is the none-zero root of the fixed-point equation, which depends on fairness ratios $\beta^{(c)}, c \in \{1, 2, \ldots, L\}$ and $n^{(M)}$.

To evaluate the effect of the fairness ratios, Fig. 4 demonstrates how $q^{(g),F}, g \in \{1, 2, M\}$, $p^{(c)}, c \in \{1, 2\}$, $R_{out}^{(g),F}$ and $R_{\max}^{F}$ vary with $\beta^{(1)}$ with $L = 2$ and $\beta^{(2)} = 3$, where $R_{out}^{(g),F}, g \in \{1, \ldots, L, M\}$, is the fairness-constrained data rate of each group, which is obtained by combining (4) and (10). Intuitively, a larger fairness ratio $\beta^{(1)}$ indicates that the single-link group 1 demands a better throughput performance, for which the transmission strategy should be aggressive with a higher transmission probability $q^{(1)}$, while the transmission strategy of the multi-link group M should be conservative. Therefore, we can see from Fig. 4(a) that with the increase of $\beta^{(1)}$, $q^{(1),F}$ grows up while $q^{(M),F}$ decreases. In the meantime, it is interesting to see that the transmission probability $q^{(2),F}$ drops as well due to a fixed fairness ratio $\beta^{(2)} = 3$ with a varying $q^{(M),F}$.

Note that the growth of $q^{(1),F}$ would lead to high group data rate $R_{out}^{(1),F}$ as shown in Fig. 4(c), and it also leads to mounting channel contention in channel 1 along with a low successful transmission probability of packets in channel 1, $p^{(1)}$, as shown in Fig. 4(b). On the other hand, for channel 2, since both $q^{(2),F}$ and $q^{(M),F}$ are reduced, the channel contention would be relieved and the successful transmission probability of packets in channel 2, $p^{(2)}$, grows. Accordingly, although the transmission probability of nodes in group 2, $q^{(2),F}$, declines, its group data rate $R_{out}^{(2),F}$, as shown in Fig. 4(c), can still be slightly improved when $\beta^{(1)} < \beta^{(2)}$.

For the fairness-constrained maximum sum rate $R_{\max}^{F}$, we can see from Fig. 4(c) that it grows with $\beta^{(1)}$ if $\beta^{(1)} < \beta^{(2)} = 3$ and declines if $\beta^{(1)} > \beta^{(2)}$, indicating that the maximum value of $R_{\max}^{F}$ is achieved when $\beta^{(1)} = \beta^{(2)}$. The above observation is extended by Corollary 1 to the general case, i.e., $L > 2$.

Corollary 1: If and only if $\beta^{(1)} = \beta^{(2)} = \cdots = \beta^{(L)} = \beta$, the fairness-constrained maximum sum rate can be optimized at $R_{\max}^{F} = e^{-1} \sum_{c=1}^{L} R_c$ and the corresponding optimal transmission probability of each group satisfies

$$\begin{cases} q^{(M),F} = \dfrac{1}{n^{(M)}(1+\beta)} \\ q^{(c),F} = \dfrac{\beta}{n^{(c)}(1+\beta)}, \end{cases} \tag{11}$$

where $c \in \{1, 2, \ldots, L\}$.

Proof: The sufficiency could be proven by substituting $\beta^{(1)} = \beta^{(2)} = \cdots = \beta$ into (10). The necessity could be proven based on the proof by contradiction, that is, with distinct fairness ratios, the optimal transmission probabilities would be different from those in Theorem 1, indicating that the maximum sum rate cannot be achieved. ■

C. Insights for Practical System Design

So far, we have obtained the fairness-constrained maximum network sum rate and corresponding optimal transmission probabilities of each group. The above analysis sheds important light on the practical system design.

Specifically, due to the coupling among single-link groups and the multi-link group, the fairness setting of one group would affect the data rate performance of all other groups, even when they are in different channels. Once a single-link group demands better data rate performance, it will impose a high

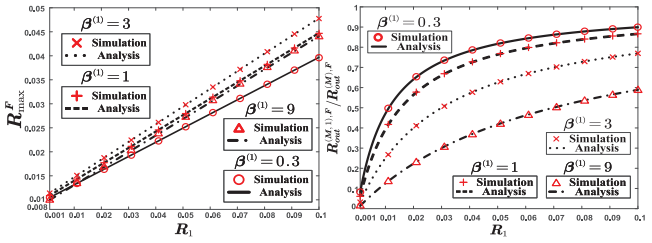

Fig. 5. (a) Fairness-constrained maximum sum rate $R_{\max}^{F}$ and (b) Data rate ratio $R_{out}^{(M,1),F}/R_{out}^{(M),F}$ versus the encoding rate R_1. The transmission probabilities of each group satisfy (10). $n^{(1)}=50, n^{(2)}=75, n^{(M)}=50$. $L=2$. $\beta^{(2)}=3$, $\beta^{(1)}\in\{0.3,1,3,9\}$. $R_2=0.03$ bit/s/Hz.

fairness ratio. Yet, as shown in Fig. 4c, where we take single-link group 1 for example, the benefit of increasing fairness ratio $\beta^{(1)}$ becomes marginal when $\beta^{(1)}$ is large. However, its side effect is severe. That is, the data rate performance of other groups and the network sum rate continue to fall. This observation along with Corollary 1 indicates that to achieve good data rate performance in a practical multi-link random access system, the fairness ratios should be carefully selected such that the variance of them is not significant.

The channel condition is another key factor in determining the data rate performance of the multi-link group. For illustration, Fig. 5 demonstrates how the fairness-constrained maximum sum rate $R_{\max}^{F}$ and the data rate ratio of the multi-link group data rate on link 1 to its total data rate, denoted as $R_{out}^{(M,1),F}/R_{out}^{(M),F}$, vary with the encoding rate on link 1, R_1, with $\beta^{(1)}=0.3,1,3$ or 9. We can see from Fig. 5(a) that better channel condition (a larger R_1) improves the overall rate performance, which can further be optimized with the same setting of the fairness ratios, i.e., in the case of $\beta^{(1)}=\beta^{(1)}=3$, as Corollary 1 suggests. On the other hand, for Fig. 5(b), we can clearly see that with better channel condition (i.e., a higher R_1) or larger share of data rate in link 1 (i.e., a smaller $\beta^{(1)}$), the data ratio $R_{out}^{(M,1),F}/R_{out}^{(M),F}$ grows, although the increasing rate becomes marginal when either R_1 is large or $\beta^{(1)}$ is small. A closer look at Fig. 5(b) shows that the data rate ratio $R_{out}^{(M,1),F}/R_{out}^{(M),F}$ would be close to zero if the channel condition in link 1 is poor or the share of data rate of the multi-link group is small. In this case, the benefit of accessing link 1 is limited and turning off the air-interface on link 1 could be the right choice in terms of energy saving without the degradation of the rate performance.

IV. Conclusion

This letter aims at optimizing the data rate performance of a multi-link slotted Aloha network, where MLDs and SLDs coexist in different channels. By characterizing the behavior of the HoL packet of each device, we obtain the steady-state point in each channel and the data rate of each single-link/multi-link group. The analysis shows that to achieve the maximum network sum rate, the transmission probabilities of each single-link/multi-link group should satisfy a set of equations. If the transmission probability of the multi-link group is selected improperly, then a severe fairness issue in terms of group data rate arises even though the maximum network sum rate is obtained.

To further ensure certain fairness among devices, the group rate fairness ratio in each channel is proposed. Explicit expressions of the fairness-constrained maximum network sum rate and corresponding optimal transmission probabilities of each group are derived. It is revealed that the fairness-constrained maximum network sum rate is lower than the unconstrained one as long as there is a difference in the fairness ratios among groups, which indicates an inherent tradeoff between efficiency and fairness. Insights of the analysis on practical system design are also discussed, which suggests that a large variance of fairness ratios on different channels should be avoided to improve the overall data rate performance, and the benefit of multi-link transmission capability crucially depends on the channel condition. A final note is that this letter focuses on the saturated condition where the network sum rate is pushed to the limit. How to extend the analysis to the unsaturated case is an interesting issue, which deserves attention in the future study.

References

[1] M. S. Ali, E. Hossain, and D. I. Kim, "LTE/LTE-A random access for massive machine-type communications in smart cities," *IEEE Commun. Mag.*, vol. 55, no. 1, pp. 76–83, Jan. 2017.

[2] N. M. Abramson, "The ALOHA system: Another alternative for computer communications," in *Proc. Fall Joint Comput. Conf.*, vol. 44, Nov. 1970, pp. 281–285.

[3] H. K. Prabu, R. Lukitowati, H. C. Kusuma, R. Harwahyu, and R. F. Sari, "Evaluating steady-state performance in narrowband Internet of Things (NB-IoT)," in *Proc. IEEE R10 Hum. Tech. Conf. (R10-HTC)*, West Java, Indonesia, Nov. 2019, pp. 211–215.

[4] O. Georgiou and U. Raza, "Low power wide area network analysis: Can LoRa scale?" *IEEE Wireless Commun. Lett.*, vol. 6, no. 2, pp. 162–165, Apr. 2017.

[5] T. Song and T. Kim, "Performance analysis of synchronous multi-radio multi-link MAC protocols in IEEE 802.11be extremely high throughput WLANs," *Appl. Sci.*, vol. 11, no. 1, p. 317, 2021.

[6] S. Naribole, S. Kandala, and A. Ranganath, "Multi-channel mobile access point in next-generation IEEE 802.11be WLANs," in *Proc. IEEE Int. Conf. Commun. (ICC)*, Montreal, QC, Canada, Jun. 2021, pp. 1–7.

[7] L. Liu, Y. Wei, Y. Bi, and J. Song, "Cooperative transmission and data scheduling mechanism of multiple interfaces in multi-radio access environment," in *Proc. IEEE GMC*, Shanghai, China, Oct. 2009, pp. 1–5.

[8] Z. Zhang and Y.-J. Liu, "Throughput analysis of multichannel slotted ALOHA systems in multiple log-normal and Rayleigh interferers environment," in *Proc. IEEE VTC-Front. Tech.*, vol. 1. Denver, CO, USA, May 1992, pp. 55–58.

[9] D. T. C. Wong, Q. Chen, X. Peng, and F. Chin, "Performance analysis of multi-channel pure collective Aloha MAC protocol for satellite uplink access," in *Proc. IEEE Reg. 10 Conf.*, Penang, Malaysia, Nov. 2017, pp. 164–169.

[10] K. Cohen and A. Leshem, "Distributed throughput maximization for multi-channel ALOHA networks," in *Proc. IEEE CAMSAP*, St. Martin, France, Dec. 2013, pp. 456–459.

[11] R. Shi and Y. Xiao, "Jamming strategy optimization for dual-channel ALOHA network with long time delay," in *Proc. IEEE ICCSN*, Chengdu, China, Jul. 2018, pp. 11–15.

[12] Á. López-Raventós and B. Bellalta, "IEEE 802.11be multi-link operation: When the best could be to use only a single interface," in *Proc. IEEE MedComNet*, Ibiza, Spain, Jun. 2021, pp. 1–7.

[13] N. Karakoç and T. M. Duman, "Rate selection for wireless random access networks over block fading channels," *IEEE Trans. Commun.*, vol. 68, no. 3, pp. 1604–1616, Mar. 2020.

[14] L. Dai, "Stability and delay analysis of buffered Aloha networks," *IEEE Trans. Wireless Commun.*, vol. 11, no. 8, pp. 2707–2719, Aug. 2012.

[15] R. Abbas, M. Shirvanimoghaddam, Y. Li, and B. Vucetic, "Random access for M2M communications with QoS guarantees," *IEEE Trans. Commun.*, vol. 65, no. 7, pp. 2889–2903, Jul. 2017.